# Characterization of Iron – Based Partial Pre - Alloyed Powders as Matrix Materials for Diamond Tools

*A Anitha* Lakshmi[1*], *P*. Srividya Devi[2], *M*. Rekha[2], *Zayd* A. Balasem

[1]Mechanical Department, Gokaraju Rangaraju Institute of Engineering and Technology, Bachupally, Hyderabad, Telangana, India.
[2]EEE Department, Gokaraju Rangaraju Institute of Engineering and Technology, Bachupally, Hyderabad, Telangana, India
Department of Refrigeration and air Conditioning Techniques engineering, College of technical engineering, The Islamic University, Najaf, Iraq.

**Abstract.** Fe-Cu-Co is a structural component used in applications requiring both high strength and high hardness. A diamond cutting tool with iron -based (Fe -53%, Cu – 28%, Co -17%, P– 1% & Ni -1%) pre-alloyed powders was prepared in the laboratory using powder metallurgy technique. Commercially available pure powders were combined to create the alloys, which were then roll compacted into bars and right away hot processed into fully dense alloy bars. Solid state sintering technique is used to manufacture composite material as it gives less defectives, more accurate than casting and excellent dimensional control. During sintering process metal powders are blended in ball milling and are compacted on hot press machine by applying heat and pressure simultaneously at different elevated temperatures. The sintered specimens are subjected to hardness, impact, density and porosity tests along with fractography study. From experimental observations it is found that material has high hardness than the steel, which can withstand mechanical vibrations, high impact strength and high toughness. According to experimental results it is most suitable for cutting applications, and there is a possibility to add diamond crystals in this tool, to strengthen hardness helping to cut the rocks.

**Keywords:** Material characterization, porosity, temperatures, hardness, green sintering

## 1 Introduction

The unique features of the matrix and the relationship between of the diamond and matrix phases impact the manner in which diamond tools perform. The matrix material must be selected with regard for the workpiece in order to achieve the best performance. Diamond retention within the matrix needs to be increased, and rate of wear of the diamond and matrix should be synchronized to encourage self-sharpening. A significant issue in the manufacture of diamond tools is selecting an appropriate matrix material. [1-3] With a good balance of

* Corresponding Author: anitha.akkireddy@gmail.com

high temperature hardness, toughness, and self-sharpening abrasiveness, cobalt base alloys have been recognized as the best matrix materials. Cobalt is a crucial strategic resource, nevertheless., [4,5] has a high and unstable pricing. Due to these issues, its use in diamond tools is being restricted, especially in middle- and low-end markets. The potential of iron-based matrixes has been extensively investigated because iron and cobalt are cognate elements with related crystal shapes and attributes. [6–10] The benefits of iron alloys are increased wettability and greater adhesion to the diamond, as well as good mechanical characteristics which includes bend strength and hardness compared to cobalt. Regular iron powders, on the contrary, have an ability to become oxidized by water vapor absorbed from the air, which reduces their strength and may result in brittleness, impairing the sintering properties. Furthermore, because the iron base matrix materials must be sintered at high temperatures and within a specific range, poor adhesion and insufficient diamond phase retention may be an issue. Iron base matrix materials exhibit poor cutting efficiency and have short in-service lifespan mostly due to this. In conjunction with allowing full application of the beneficial characteristics of iron base materials, the invention of new iron matrix materials,[11–13] and novel techniques for producing these powders,[14] could help lessen the disadvantages in the sintering and cutting processes that were previously discussed. This strategy has shown to be successful and is frequently utilized for medium- and low-cost diamond tools. In this paper the main objective of work is experimentally evaluating the mechanical properties of composite material manufactured by solid state sintering process using metal powders (Fe-Cu based powders) [12] and compare and conclude the results to show the properties vary with respect to temperatures.

## 2 Methodology and fabrication:

Several techniques have been developed which permit large production rates of powdered particles, often with considerable control over the size ranges of the final grain population. Powders were prepared by crushing, grinding, chemical reactions, or electrolytic deposition. The most commonly used powders are iron-base materials. Powders of the metals Ferrous - 53%, copper-28%, cobalt -17%, phosphorous -1%, and nickel -1%. with mesh size (45 microns) are kept inside the ball milling for thorough mixing as represented in Fig. 1. Binders such as wax or thermoplastic polymers are added to improve green strength to make a homogeneous mass with uniform distribution of particle size and composition the combining is generally carried in air / inert gases to avoid the oxidation After mixing we have obtained a powder with desired green strength mixing, and lubricants are added along with powders for improving flow characteristics.


**Fig. 1** (a) Metal powder (b) rotary drum

The mould is prepared by filling the metal powders weighing 50 grams as shown in Fig. 2 into the two die cavities, Close the die cavity with plungers, to check whether the die is properly fitted or not. The electrodes (Fig. 2) are placed upon the die and die setup is placed between hot pressing machine jaws as illustrated in Fig. 3. The temperature 850 ℃ is setup in temperature digital panel, a pressure of 30 bar is setup in pressure gauge, sintering time is setup for 5min for first two specimens. The lower jaw of the machine is fixed and upper jaw will compress the dies with help of electrode for good compaction.


**Fig. 2.** Representation of calibration of powders and Electrode

The heat is transferred to dies with the help of heating electrodes reaching to the setup temperature where pressure is applied till the sintering time. After completion of sintering time (5mins) , the upper jaws opened to remove the die from hot press. After cooling the specimens are removed from die cavities.

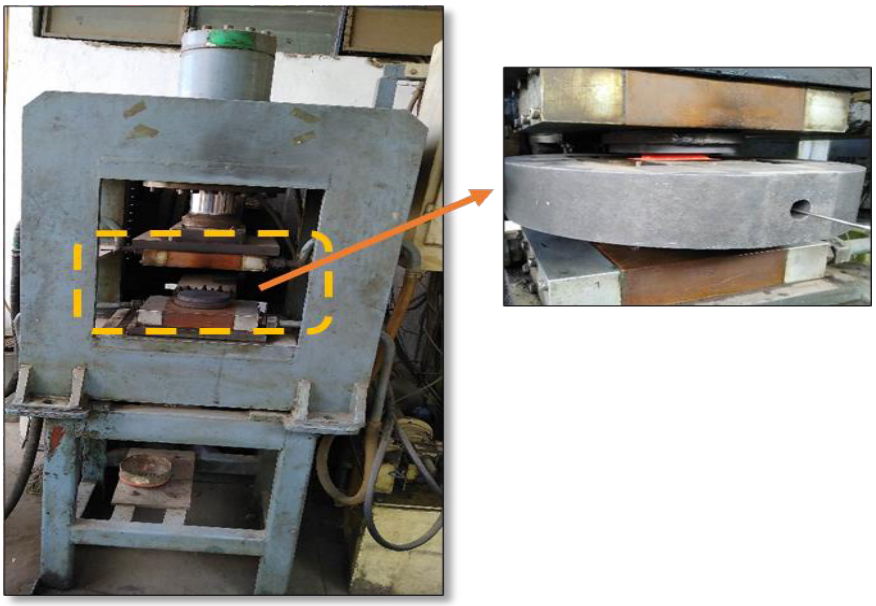

**Fig. 3.** Hot Press Green Sintering Machine

The specimen dimensions of width 10 mm, height 10 mm and length 55 mm are prepared. At a time two specimens are powder metallurgic from hot press. The similar setup is repeated for remaining specimens by varying the input temperatures as represented in Table 1 at constant pressure and sintering time. The complete flow of the process is shown in the Fig. 4

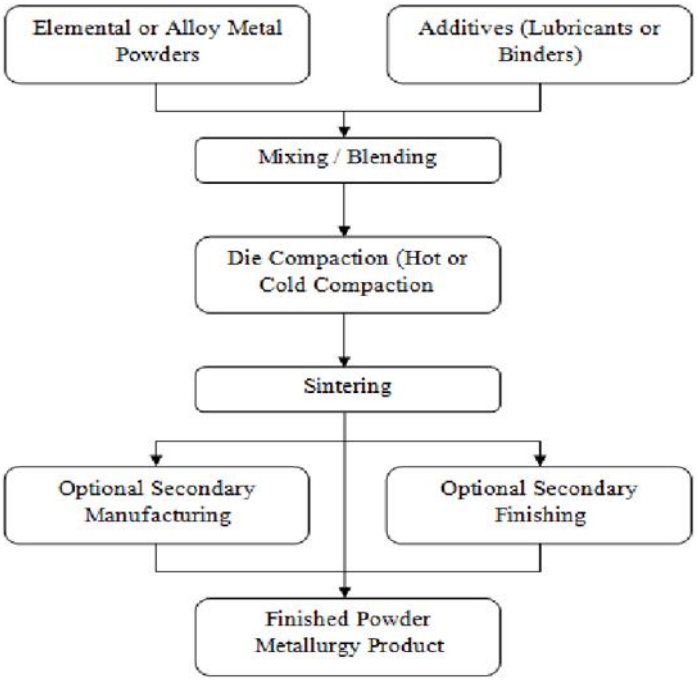


**Fig. 4.** Methodology Line diagram

**Table1:** Experiments conducted on Hot Press Green Sintering Machine.

| Exp. No. | No. Of Specimens | Temperatures in (°C) | Pressure in (Bar) | Sintered Time in (Min) |
|---|---|---|---|---|
| 1 | 2 | 850 | 30 | 5 |
| 2 | 2 | 800 | 30 | 5 |
| 3 | 2 | 750 | 30 | 5 |
| 4 | 2 | 700 | 30 | 5 |

**Fig. 5:** Sintered specimens.

## 3 Experimentation:

The porosity of the specimens is determined by calculating theoretical, Relative sintered Density mathematical expressions Calculation of Theoretical and Relative Sintered Density: The bulk and Apparent densities, open porosity of the samples is measured using the Archimedes' technique with water as the immersing medium. The relative density is obtainable with respect to the theoretical density Eq.2. Sample calculation is shown below Eq.3.The theoretical density is estimable using the rule of mixtures, based on starting compositions of the samples and following pure component densities as shown in the Eq.1. To calculate the theoretical sintered density of composite material.

**Table 2:** Chemical composition and theoretical density

| Sr. No. | Metal Powder | % Metal Powder Used | Density in (gm/cc) |
|---|---|---|---|
| 1 | Ferrous | 53 | 7.874 |
| 2 | Copper | 28 | 8.96 |
| 3 | Cobalt | 17 | 8.86 |
| 4 | Phosphorous | 1 | 1.89 |
| 5 | Nickel | 1 | 8.9 |

Theoretical sintered density = 100/(53/7.874+28/8.96+17/8.86+1/1.89+1/8.9)

$=100/(6.74+3.125+1.91+0.54+0.11)=8.052 g/cm^3$ Eq.1

$$\text{Relative density}=\frac{\text{weight of specimen in air}}{\text{volume of the specimen}} \quad \text{Eq. 2}$$

**At 700℃**

Length of the specimen (L) = 54.63 mm

Width of the specimen (W) = 9.96 mm

Height of the specimen (H) = 11.05 mm

Volume of the specimen =L*W*H = 54.63×9.96 x11.05 =6.01 gm/cc Eq.3

$$\rho_{700} = \frac{48.496}{6.01} = 8.06 \text{ gm/cc}$$

**Table 3.** Relative density

| Sr. No. | Temperatures in | Weight In Air | Volume | Density |
|---|---|---|---|---|
| 1 | 850 | 49.763 | 6.307 | 7.89 |
| 2 | 850 | 50.30 | 6.235 | 8.06 |
| 3 | 800 | 49.565 | 6.26 | 7.91 |
| 4 | 800 | 49.642 | 6.23 | 7.96 |
| 5 | 750 | 48.474 | 5.97 | 8.11 |
| 6 | 750 | 49.663 | 6.11 | 8.11 |
| 7 | 700 | 48.496 | 6.01 | 8.06 |
| 8 | 700 | 48.947 | 6.13 | 7.97 |
| Average Relative Density | | | | 8.008 |

Green density test: The relevant attributes of compacts include density and strength, in addition to dimensions, which are of course very significant in the fabrication of individual PM parts. The so-called "green density" has a significant impact on "green strength" and has the potential to change the "final," or sintered, density. The Archimedes principle determines

it. The phrase "green strength" is used to describe a compact's durability. Green density is calculated as the ratio of weight of the specimen in air to the difference of weight of specimen in air and weight of specimen in water using Eq.4.

The specimens are kept inside the box and immersed in the water tub and water tub is placed under the electronic weighing machine tied to a weighing rope which helps to hold the specimens inside the tub as shown in Fig. 6. The weight of the specimens in water is measured. By Repeating the same procedure for remaining specimens, the values are noted.

$$\text{Green density} = \frac{\text{weight of specimen in air}}{\text{Weight of specimen in air} - \text{weight of specimen in water}} \quad \text{Eq.4}$$

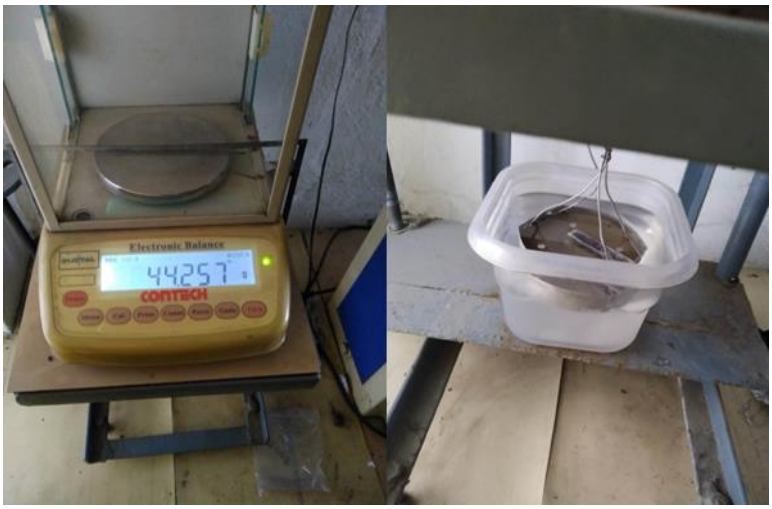


**Fig. 6.** Electronic balance machine and water tub with specimens immersed

**Table 4:** Experimental observations of Green density test

| Sr. No | Temperature in (ºC) | Weight of specimen in air (g) | Weight of specimen in water (g) | Difference (g) | Sintered Density (g/cc) |
|---|---|---|---|---|---|
| 1 | 850 | 49.763 | 43.574 | 6.185 | 8.040 |
| 2 | 850 | 50.301 | 44.017 | 6.284 | 8.004 |
| 3 | 800 | 49.565 | 43.402 | 6.163 | 8.042 |
| 4 | 800 | 49.642 | 43.475 | 6.167 | 9.049 |
| 5 | 750 | 48.474 | 42.450 | 6.024 | 8.046 |
| 6 | 750 | 49.663 | 43.492 | 6.171 | 8.047 |
| 7 | 700 | 48.496 | 42.468 | 6.028 | 8.045 |
| 8 | 700 | 48.947 | 42.862 | 6.085 | 8.043 |
| Average Relative Density | | | | | 8.16 |

## 4 Results and Discussions

**Porosity test: Porosity** is the value used to describe how much empty, or void, space is present in a given sample and calculated using Eq. 5. Low porosity minimizes or inhibits the entry of corrosive materials into your components and is frequently correlated with enhanced

mechanical and magnetic qualities. The percentage of porosity is less with the increase in temperature as listed in Table 5

Porosity = 1 - (Theoretical Sintered Density / Actual Sintered Density) ×100 Eq.5

**Table 5:** Experimental results of porosity test

| Sr. No | Temperature in (ºC) | Theoretical Sintered Density in (g/cc) | Actual Sintered Density in (g/cc) | % Porosity |
|---|---|---|---|---|
| 1 | 850 | 8.052 | 8.040 | 0.19% |
| 2 | 850 | 8.052 | 8.041 | 0.17% |
| 3 | 800 | 8.052 | 8.042 | 0.12% |
| 4 | 800 | 8.052 | 8.049 | 0.068% |
| 5 | 750 | 8.052 | 8.046 | 0.12% |
| 6 | 750 | 8.052 | 8.047 | 0.11% |
| 7 | 700 | 8.052 | 8.045 | 0.13% |
| 8 | 700 | 8.052 | 8.043 | 0.15% |

**Hardness test:** Using a Rockwell hardness machine and following ASTM standards, the hardness of the sintered specimens was measured. In the test to ascertain the specimens' hardness, a 5 kg load was applied. Each specimen underwent three trials during the test. Table 6 displays the average values and observed values for three trials. Figure 7 shows a graphic representation of the hardness test. The graphic unequivocally demonstrates that the harder carbon particles make the hardness rise with temperature, from 100 HRB to 105.5 HRB. Hardness increases by 25% when going from 0% to 10%.

**Table 6:** Experimental results of Rockwell test

| Sr. No | Temperature in (ºC) | Hardness 1 (HRB) | Hardness 2 (HRB) | Average (HRB) |
|---|---|---|---|---|
| 1 | 850 | 105 | 106 | 105.5 |
| 2 | 850 | 106 | 104 | 105 |
| 3 | 800 | 102 | 103 | 102.5 |
| 4 | 800 | 102 | 104 | 103 |
| 5 | 750 | 102 | 102.6 | 102.3 |
| 6 | 750 | 104 | 100 | 102 |
| 7 | 700 | 102 | 103 | 102.5 |
| 8 | 700 | 101 | 99 | 100 |

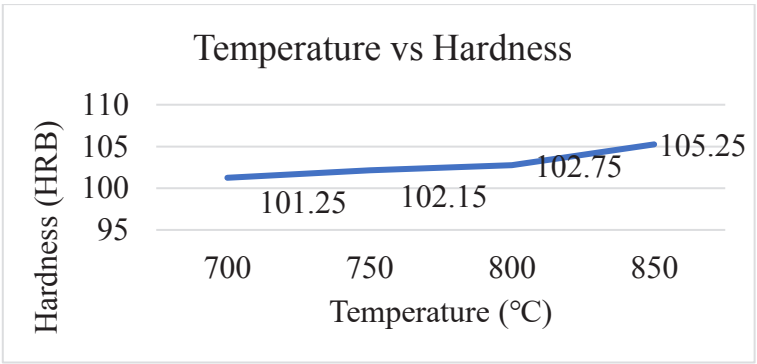


**Fig. 7.** Graphical representation of temperature vs hardness graph

**Impact Test:** Impact test determines the amount of energy absorbed by a material during fracture. This absorbed energy is a measure of a given material's toughness and acts as a tool to study temperature-dependent brittle-ductile transition. The impact energy is used to analyse whether the material is brittle or ductile in nature. The Energy absorbed before fracture values of the green sintered specimens with respect to temperatures are listed in Table 7. From the Fig.8 with the increase in temperature the impact strength is increasesThe material has high strength to withstand mechanical vibrations and have greater toughness then "HSS steel".

**Table 7:** Experimental observations of impact test

| Sr. No | Temperature in (°c) | Impact Energy of specimen1 in Joule (J) | Impact Energy of specimen2 in Joule (J) | Average Impact Energy in Joule (J) |
|---|---|---|---|---|
| 1 | 850 | 10 | 6 | 8 |
| 2 | 800 | 8 | 4 | 6 |
| 3 | 750 | 7 | 5 | 6 |
| 4 | 700 | 5 | 3 | 4 |

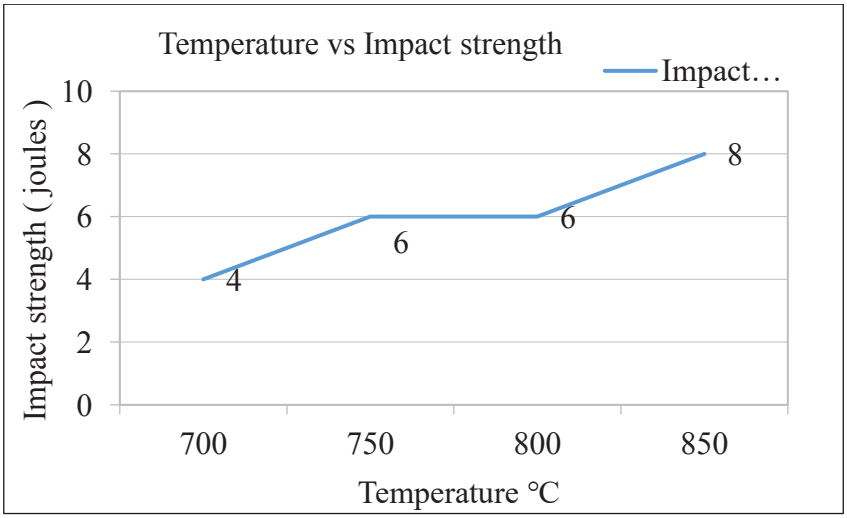


**Fig. 8.** Graphical representation of temperature vs hardness graph

**Microstructure:** Fig. 9 (a) to (d) show the SEM image of composite alloy. It is clearly evident that the homogenous distribution of powders is seen. It is observed in Fig. 9(a) & (b) that the bonding strength of alloy particles is increased due to elevated temperature maintained at 850 °C in the sintering process. The large void present in the surface is due to the poor flow characteristics of metal powder during compaction. It is observed that the crystal structures are changed with increase in temperature. It is found that carbon deposit molecules are more in 850°C compared to other specimens.

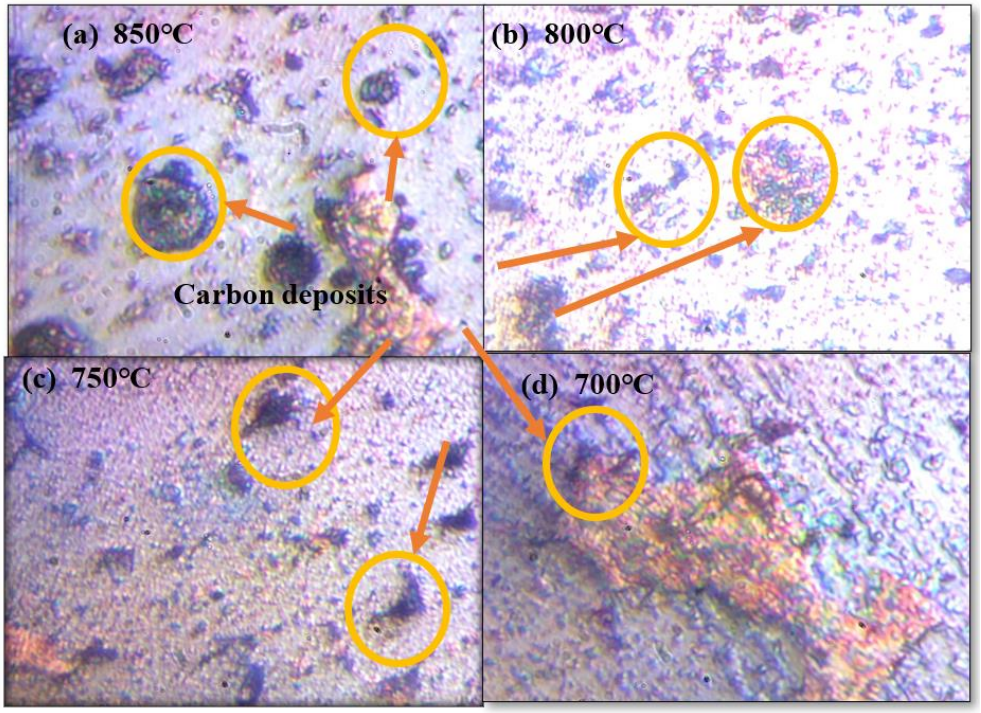


**Fig. 9.** Microstructure of the alloy at different sintering temperatures

## 6 Conclusions

The typical way of preparing metal matrix powder in the diamond tools sector is the EMMM process, which is difficult to achieve the pre-alloyed powder matrix and easily leads to powder oxidation, inhomogeneous matrix composition and solute segregation. There is poor control force between matrix material and stone, resulting in weak mechanical properties of stone devices, and limited service. To avoid this matrix of materials in powder form are taken which are blended to form alloyed mixture and sintered to form alloy specimen which will be characterised for further calculations. The relative density, porosity of matrix sintered segments prepared using the Hot press sintering process powder are greatly improved compared with those available tools. The sintering temperature of the diamond tools is reduced as well as the diamond graphitization at high temperatures, when using the pre-alloyed powder. In addition, the mechanical properties of the diamond tools are also greatly improved. The Hardness and impact strength of the alloy is increased drastically with temperature.

## References

1. L. Zhang, Y. Sun, M. Liu, M. Liu, L. Wang, Research on the influence of cutting parameters on chips in the process of diamond bead cutting pipeline steel, Diam. Relat. Mater. **111** (2021), 108220.
2. W.W. Steven, Diamond retention in sintered cobalt bonds for stone cutting and drilling, Diam. Relat. Mater. **8** (1999) 2043–2052.

3. S. Kannan, A. Kishawy, I.M. Deiab, M.K. Surappa, On the role of reinforcements on tool performance during cutting of metal matrix composites, J. Manuf. Process. **8** (2006) 67–75,
4. p. u. t. d. o. t. A. I. H. Committee, ASM Handbook. Volume 7, Powder Metal Technologies And applications, ASM International, Materials Park, OH, 1998.
5. A. Di Ilio, A. Togna, A theoretical wear model for diamond tools in stone cutting, Int. J. Mach. Tools Manuf. **43** (11) (2003) 1171–1177.
6. P.A. Loginov, U.A. Zhassay, Ya M. Bychkova, M.I. Petrzhik, S.K. Mukanov, D.A. Sidorenko, A.S. Orekhov, S.I. Rupasov, E.A. Levashov, Chromium-doped Fe-coNi binders for diamond cutting tools: the features of the structure, mechanical properties, and adhesion to diamond, Int. J. Refract. Met. H **92** (2020), 105289.
7. J. Li, W. Fang, L. Wan, X. Liu, W. Hu, D. Cao, K. Han, Y. Li, Y. Yan, Research on the bonding properties of vitrified bonds with porous diamonds and the grinding performance of porous diamond abrasive tools, Diam. Relat. Mater. **123** (2022), 108841,
8. Z. Su, S. Zhang, L. Liu, J. Wu, Microstructure and performance characterization of co-based diamond composites fabricated via fused deposition molding and sintering, J. Alloys Compd. **871** (2021), 159569,
9. V.V. Tkatchenko, V.P. Filonenko, R.K. Bagramov, I.P. Zibrov, A.S. Anokhin, I.V. Bondar, M.A. Andrianov, A.N. Shipkov, Diamond composites with Al-co binder:synthesis, structure, wear resistance, Mater. Lett. **330** (2023), 133317,
10. H. Ting, T. Cheng, S. Chung, T. Chi, Y. Horng, Tribological behaviours of the diamond-coated cemented carbide tools with various cobalt contents, Diam. Relat. Mater. **1** (1992) 594–599,
11. Q. Zou, W. Gong and X. Zeng: 'Febased diamond tool matrix composites with a rare-earth element', J. Superhard Mater., 2009, (**12**), 407–412.
12. He Dai, Liming Wang, et al.: 'Study on new type of iron–copper pre-alloyed powder materials and property', Diamond Abrasives Eng., 2013, (**4**), 15–17.
13. A. Mancisidor, C. Luno-Bilbao, N. J. Vielma, J. M. Sanchez and I. Iturriza: 'Effect of sintering atmosphere on densification, mechanical properties and diamond stability of prealloyed diamond impregnated composites obtained by free sintering', Powder Metall., 2013, **56**, 362–373.
14. G. Walther, T. Bu¨ ttner, B. Kieback, T. Weißga¨ rber, M. Hoffmann and G. Bachmann: 'Properties and sintering behaviour of fine spherical iron powders produced by new hydrogen reduction process', Powder Metall., 2014, **57**, 176–183.